AIRFOIL AERODYNAMICS

NAME: Jagdeep Singh (250911825) **LAB REPORT-2**

Introduction:

It is the study of how the fluid interacted with the moving bodies. Aerodynamics mainly a study of drag and lift forces which is due to the air passing over the solid moving body. We focused our study mainly on aerodynamics of aerofoil in this lab manual. In aerofoil theory, there are main four forces acting over the body that is lift force produced by pressure difference above and below the aerofoil, weight of the body, drag force and thrust force. Drag force, which is originated mainly from the two components that are the skin friction and pressure drag. For the streamlined bodies, the skin friction is more dominant than the pressure drag. On the other hand, the pressure drag is more dominant in case of blunt bodies due to the separation of flow from the body. The thrust force is provided by the engines to overcome the drag force and lift is produced by aerofoil to balance the weight of the aeroplane. The main configuration of the aerofoil is shown in the [1]Fig. (1).

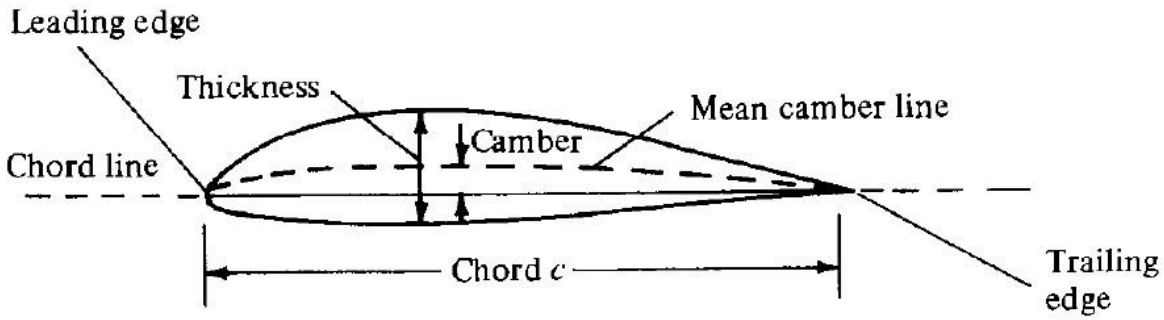

Fig. (1)

The aeroplane is moving with some velocity the forces that are acting on the aerofoil are shown in [1]Fig. (2)

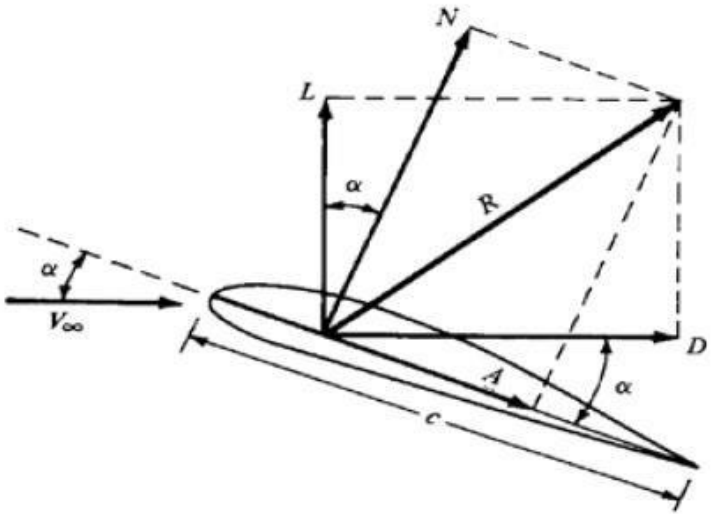

Fig. (2)

From the Fig. (2), The lift force is the component of R that is perpendicular to the free stream velocity. The drag force component of the R that is parallel to the free stream velocity. normal force component of the R that is perpendicular to the chord. Axial force component of the R that is parallel to the Chord and α is the angle of attack.

Our team has done the experimental studies on the Clark Y aerofoil configuration in the wind tunnel in the university of western Ontario. The focus of the experimental studies was to determine the lift forces and drag forces through pressure distribution, load cell data and circulation criterion on different angle of attacks. Pressure distribution can be found from pressure sensor tapping that are installed on the aerofoil and acquisition of data was obtained directly on computer. The experimental setup of the aerofoil with mounting mechanism and the angle of attack can be adjusted with screw installed on the mechanism as shown in the [2]Fig. (3).

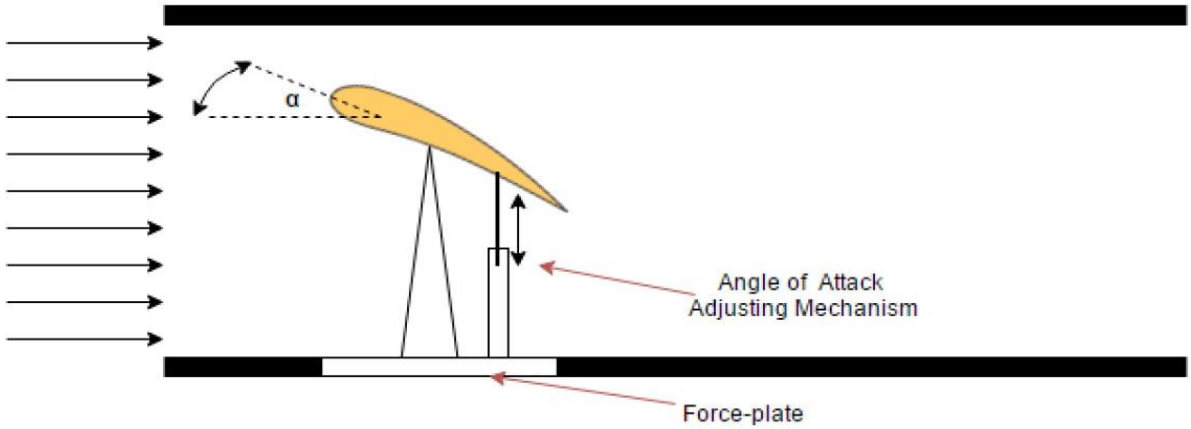

Fig. (3) Experimental Setup

The aerofoil used in the experiment was a Clark Y design. This is a flat bottomed cambered profile. The span of the wing is 40 cm; Chord length of the aerofoil is 9 inch and 1 inch is the thickness of the aerofoil. Sensors taps are separated by 1.125 inches along the chord length. The pitot static tube is used to calculate the free stream velocity. The pressure distribution and load cell data is directly obtained from the computer and for calculation of lift force from circulation concept we have been provided the MATLAB data of the polynomial function which is the order of 9 for the both the upper and lower surface.

Results and Discussions:

The drag force and lift force components are obtained from pressure distribution, load cell data and circulation criterion. The pressure distribution and load cell data were collected through the pressure sensor and load cell, respectively. Velocity distribution at different angle of attacks was calculated through Bernoulli's equation, which was the line integral over the closed contour resulting in the circulation. By Kutta-Jowaski Theorem, the lift force was computed from the formula given as:

$$l = \rho v \Gamma \, \mathrm{b}$$

Where, Γ is the circulation;

ρ, v are density and velocity of the free-stream air.

1) Table 1. Shows the time averaged values of drag and lift forces in newton. These tabulated values are obtained from load cell during experiment.

Table 1. Variation of Drag and Lift Force

Angle of Attack (Deg.)	**Drag Force (F_D)**	**Lift Force (F_L)**
0	1.01	5.34
2	1.01	6.45
4	1.38	8.54
6	1.44	8.29
8	1.54	9.43
10	1.63	9.22
12	1.9	10.35
14	3.03	8.08
16	3.18	8.13
18	3.52	8.08
20	3.83	8.36
30	6.22	9.35

2) The drag coefficient (C_D) for each angle of attack can be obtained by equation (1).

$$C_D = \frac{2F_D}{\rho {V_\infty}^2 A} \qquad \text{Eq. (1)}$$

Where,

Area of airfoil (A)= chord length * wing span

Area of airfoil (A)= (9*0.0254) *0.4= 0.09144 m^2

The free stream velocity can be evaluated using equation (2).

$$V_\infty = \sqrt{\frac{2*g*\Delta h*\rho_{water}}{\rho_{air}}} \qquad \text{Eq. (2)}$$

Where,

Density of Water, ρ_{water} = 998.2 kg/ m^3

Acceleration due to gravity, g=9.81 m/ s^2

Density of Air, ρ_{air}=1.2754 kg/m^3

Δh = Difference in the manometric Height

All fluid properties are considered at 20 ^{0}C.

For free stream velocity difference in manometric height is provided in the data set is 6.5 mm and by using Eq. (2), the free stream velocity (V_∞) is evaluated at Δh = 6.5 mm is 9.99 m/s.

The drag force is the time averaged value of data obtained from load cell and drag force of the mounting is **subtracted** from each value of drag force at different angle of attacks and corresponding lift force is calculated using Eq. (2) and the data is tabulated in the Table (2).

Table 2: Drag coefficient for each angle of attack

Angle of Attack (Deg.)	Drag Force (F_D)	Coefficient of Drag Force(C_D)
0	0.775	0.133
2	0.775	0.133
4	1.145	0.197
6	1.205	0.207
8	1.305	0.224
10	1.395	0.240
12	1.665	0.286
14	2.795	0.480
16	2.945	0.506
18	3.285	0.565
20	3.595	0.618
30	5.985	1.029

3) The lift force is evaluated from the load cell data and further lift coefficient is calculated for each angle of attack by using Eq. (3) and Lift force and Lift force coefficient data is tabulated in the Table (3) for each angle of attack. The drag force (0.235 N) of mounting is subtracted from each value of the tabulated lift force shown in Table (1) and new values of lift force is tabulated in the Table (3) and the corresponding lift force coefficient is calculated based on the subtracted values of lift force.

$$C_L = \frac{2F_L}{\rho {V_\infty}^2 A} \qquad \text{Eq. (3)}$$

Table 3: Lift coefficient for each angle of attack

Angle of Attack (Deg.)	**Lift Force**(F_L)(N)	**Coefficient of Lift Force**(C_L)
0	5.11	0.878
2	6.22	1.068
4	8.31	1.428
6	8.06	1.385
8	9.20	1.581
10	8.99	1.544
12	10.12	1.739
14	7.85	1.348
16	7.90	1.357
18	7.85	1.348

20	8.13	1.397
30	9.12	1.567

4) The pressure distribution is obtained from pressure sensors that are installed on different locations on the upper and lower surfaces of an aerofoil. There are total 17 sensors installed on an aerofoil. The pressure distribution readings are evaluated by taking time averaging of all the pressure readings for the upper and as well as lower surface. The net pressure distribution is calculated by using Eq. (4) for each angle of attack and the results are tabulated in the Table (4).

$$P_{net} = P_{lower} - P_{upper} \qquad \text{Eq. (4)}$$

Table 4: Pressure distribution on the airfoil

Angle of Attack	**Pressure Distribution (N/m^2)**
0	262.65
2	294.37
4	418.22
6	421.36
8	447.74
10	461.00
12	475.67
14	381.93
16	389.02
18	394.50
20	411.44
30	624.42

5) We know that the lift force is calculated from the area under the curve of pressure over the upper and lower surfaces. The geometry of an aerofoil is not symmetric. Hence, the geometry is split into small parts to perform numerical integration. For numerical integration, the Trapezoidal method is used. MATLAB is used to perform the numerical integration. Mathematical modelling and MATLAB code is represented in Eq. (5) to Eq. (8)

$$F_{lower} = \int P_{lower}\, dA \qquad \text{Eq. (5)}$$

$$F_{upper} = \int P_{upper}\, dA \qquad \text{Eq. (6)}$$

$$F_{lift} = F_{lower} - F_{upper} \qquad \text{Eq. (7)}$$

MATLAB Script shown below, is used for evaluating the lift force from pressure distribution data at each angle of attack and data is tabulated in the Table (5).

```
>> pmean=mean(X0degpressure(:,2:17)); %Evaluating the Mean of the pressure data at 0 degree
>> pupper=[pmean(1:8),pmean(1,16)];     %Creating the Matrix for pressure for Upper surface
>> plower=[pmean(1,1),pmean(1,9:16)];   %Creating the Matrix for pressure for Upper surface
>> liftforce0deg=0.4*trapz(chord,abs(pupper-plower)) %Numerical Integration method
liftforce0deg =3.0494                                %Results for 0 degree Lift
```

chord is defined in a MATLAB

```
chord= [0 0.028575 0.05715 0.085725 0.1143 0.142875 0.17145 0.2 0.2286] %vector of 1x9 (Meters)
```

Similarly, same script is used to calculate the lift force at each angle of attack by choosing pressure distribution at respective angles.

Table 5: Lift force and lift coefficient at different angle of attack

Angle of Attack (Degree)	**Lift Force(N)**	**Lift Force Coefficient(C_L)**
0	3.049	0.524
2	3.369	0.579
4	4.780	0.822
6	4.829	0.830
8	5.138	0.884
10	5.306	0.912
12	5.437	0.935
14	4.365	0.751
16	4.446	0.765
18	4.509	0.775
20	4.703	0.809
30	7.137	1.227

6) Circulation is the line integral of the velocity vector field around a closed curve. The circulation is represented in Eq. (9)

$$\Gamma = \oint \vec{V}.\overrightarrow{ds} \qquad \text{Eq. (9)}$$

In this experimentation, the velocity vector field is calculated from the pressure distribution by applying Bernoulli's equations which is expressed in Eq. (10)

$$V_2 = \sqrt{\frac{2*(P_2-P_1)}{\rho}} \qquad \text{Eq. (10)}$$

At leading edge velocity is 0.

The main task in circulation is to perform the line integral along the closed curve. The numerical integration is used to calculate the circulation. A ninth order polynomial function is provided for both the upper and lower surface. From the polynomial, we can calculate the small element length and can proceed with the numerical integration.

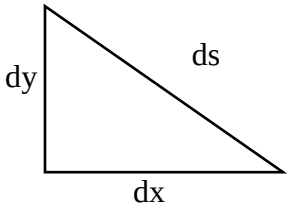

From above Fig., we can write the following expression as shown in Eq. (11)

$$ds = dx\sqrt{1 + \left(\frac{dy}{dx}\right)^2} \qquad \text{Eq. (11)}$$

The dx is calculated from the "Polyval" function in the MATLAB and "Polyder" function is used to calculate $\left(\frac{dy}{dx}\right)$ the derivative of the polynomial function. So, the circulation can be expressed as shown in Eq. (12)

$$\Gamma = \int V\sqrt{1 + \left(\frac{dy}{dx}\right)^2}\, dx \qquad \text{Eq. (12)}$$

The MATLAB script is given below which is used to calculate the circulation at each angle of attack.

```
%Upper Surface Circulation
y=polyval(polyupper,chord,[],muUpper);
z=polyder(polyupper);
ds=(1+(z).^2).^0.5;
velu0f=ds.*vupper0;
cir0u=trapz(y,velu0f);

%Lower Surface Circulation
yl=polyval(polylower,chord,[],muLower);
zl=polyder(polylower);
ds=(1+(zl).^2).^0.5;
velu0fl=vlower0.*ds;
cir0l=trapz(yl,velu0fl);
```

This script is used for each angle of attack to perform the calculation of circulation over an aerofoil. The Table (6) shows the tabulated data of circulation at each angle of attack. Once the circulation is known we can perform the calculation for the lift force. The lift force from circulation is calculated by using Kutta-Jowaski theorem which is expressed in Eq. (13)

$$F_L = \rho V \Gamma b \qquad \text{Eq. (13)}$$

The values for lift force and corresponding coefficient of lift force is calculated and tabulated in the Table (7).

Table 6: Circulation at each angle of Attack

Angle of Attack	Circulation
0	1.26
2	1.25
4	1.42
6	1.36
8	0.813
10	0.900
12	0.650
14	1.155
16	1.011
18	0.820
20	0.432
30	0.443

7) The lift force and coefficient of lift force is calculated using Eq. (13) and Eq. (3).

From Eq. (13),

$$F_L = \rho V \Gamma b$$

Where;

ρ, Density of the air

v, Free stream velocity= 9.99 m/s,

b, wing span= 0.4 m.

Table 7: Lift force and lift coefficient Evaluated from Circulation

Circulation			
Angle of Attack	**Circulation**	**Lift Force(N)**	**Lift Coefficient**
0	1.2606	6.42	1.104
2	1.2525	6.38	1.097
4	1.4203	7.24	1.244
6	1.3611	6.93	1.192
8	0.8136	4.15	0.713
10	0.9	4.59	0.788
12	0.65	3.31	0.569
14	1.1554	5.89	1.012
16	1.0118	5.16	0.886
18	0.82	4.18	0.718
20	0.4326	2.20	0.379
30	0.4434	2.26	0.388

8) Fig. (4) shows the drag coefficient variation with the angle of attack. The drag coefficient is obtained from load cell data. The Fig. (4) shows that drag coefficient increases with the increase of angle of attack.

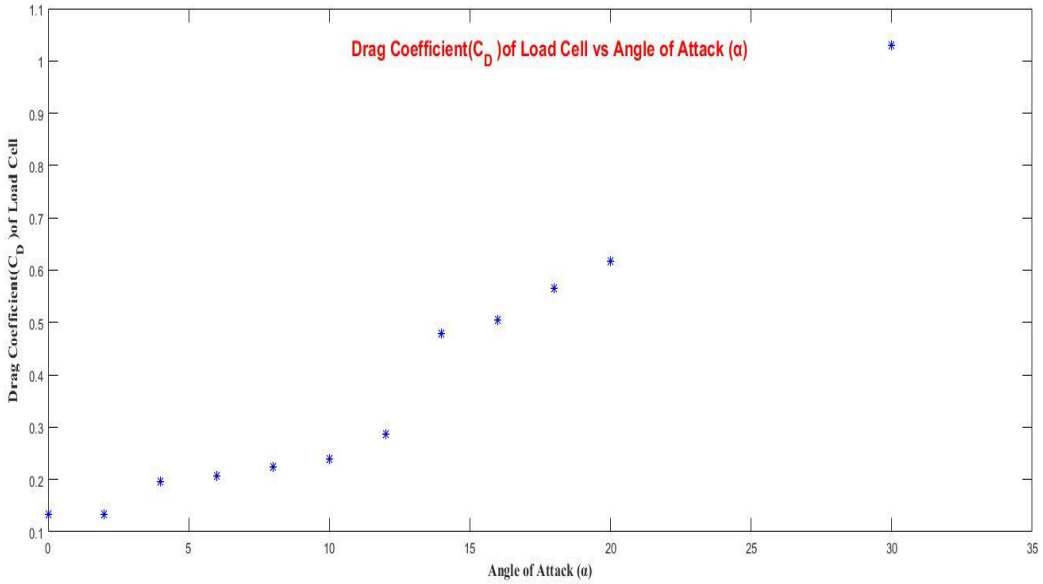

Fig. 4: Drag coefficient variation with angle of Attack (Load Cell)

9) Fig. (5) shows the variation of coefficients of lift which are calculated from three different method namely load cell, pressure distribution and circulation with the angle of attack. The plot of lift coefficient obtained from the circulation and pressure distribution with angle of attack is shown in fig. 5.

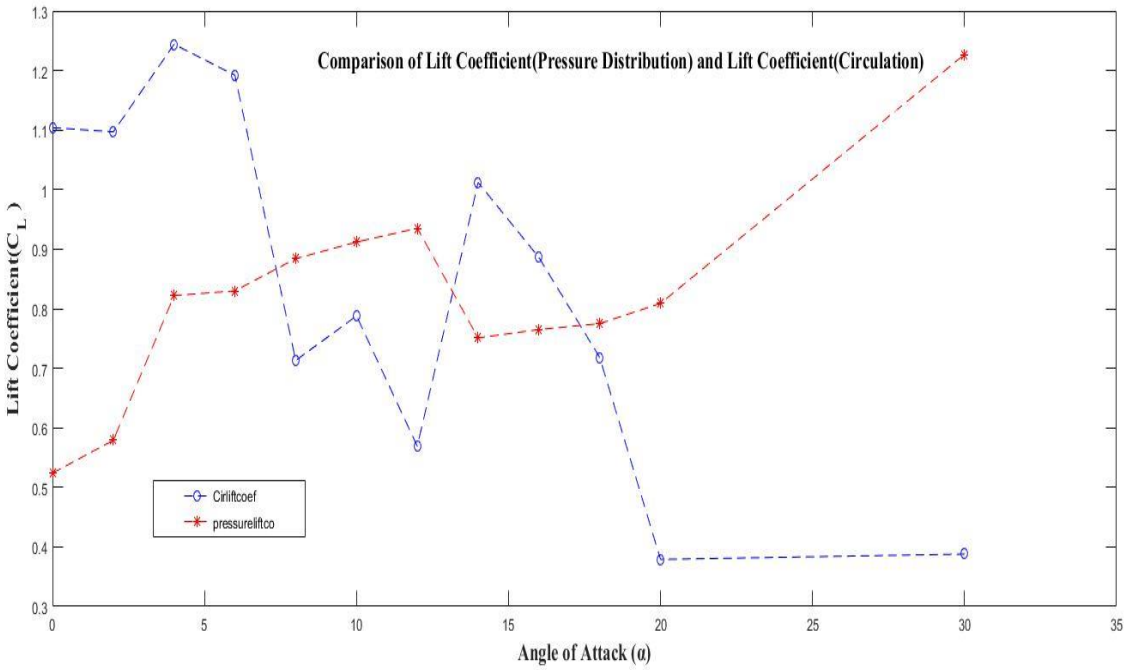

Fig. 5: Circulation and pressure distribution lift coefficient

10) Table (8) shows the tabulated data of C_L/C_D ratio evaluated from load cell, pressure distribution and circulation data with angle of attack. The drag coefficient is only calculated from Load cell data. Fig. (6) shows the corresponding variation of C_L/C_D with the angle of attack.

Table 8: C_L/C_D ratio from three different Method

Angle of Attack(α)	**C_L/C_D (Circulation Data)**	**C_L/C_D (Pressure Distribution)**	**C_L/C_D (Load Cell Data)**
0	8.30	3.94	6.60
2	8.25	4.35	8.03
4	6.31	4.17	7.25
6	5.76	4.01	6.69
8	3.18	3.95	7.06
10	3.28	3.80	6.43
12	1.99	3.27	6.08
14	2.11	1.56	2.81
16	1.75	1.51	2.68
18	1.27	1.37	2.39
20	0.61	1.31	2.26
30	0.38	1.19	1.52

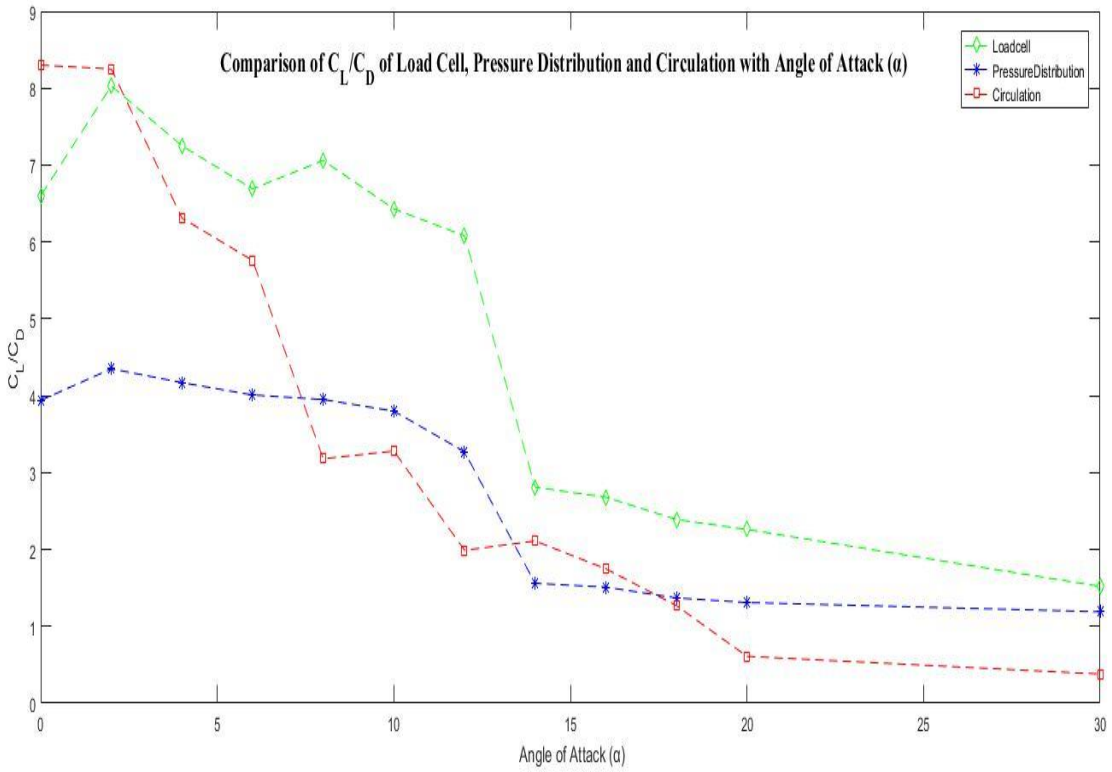

Fig. (6) Variation of C_L/C_D for three different method with angle of attack

11) Table (9) shows the percentage difference in the values of lift forces calculated from pressure distribution and circulation and load cell data.

Table 9: Percentage difference of Lift forces

Angle of Attack	**Lift Force(N) Circulation**	**Lift Force(N) Load Cell**	**Lift Force(N) Pressure Distribution**	**%Difference Load cell and Pr. Distribution**	**%Difference Load cell and Circulation**
0	6.42	5.11	3.049	40.33	20.44
2	6.38	6.22	3.369	45.84	2.53
4	7.24	8.31	4.78	42.48	12.92
6	6.93	8.06	4.829	40.09	13.96
8	4.15	9.2	5.138	44.15	54.94
10	4.59	8.99	5.306	40.98	48.99
12	3.31	10.12	5.437	46.27	67.28
14	5.89	7.85	4.365	44.39	25.01
16	5.16	7.9	4.446	43.72	34.75
18	4.18	7.85	4.509	42.56	46.78
20	2.20	8.13	4.703	42.15	72.89
30	2.26	9.12	7.137	21.74	75.23

12) **Comments:**

a) From the Table 1. It can be clearly seen that the lift force increases as the angle of attack increases. The highest lift force is obtained when the angle of attack is 12 degree. However, with further increase in the angle of attack the lift force decreases because the velocity over the upper surface starts to decrease and due to which pressure increases on the upper surface by Bernoulli's theorem and opposite trends happened on the lower surface. When the angle of attack is 30 degree, the velocity is minimum which is the minimum flight velocity on which the flight sustains and corresponding angle of attack where the velocity is minimum is known as the stall angle. On the other hand, as the angle of attack increases, the flow begins to separate from the upper surface of the airfoil at its trailing edge. This separated flow causes the onset of downwash and increases the drag force significantly. This separation of the flow increases as the angle of attack increases. When the lift producing, downwash is fully replaced by swirling vortices of air, lift force begins to decrease. At this point, the aerofoil is stalled and the angle of attack when the stall begins is called the critical angle of attack.

b) Table (9) shows the variation of lift forces calculated form pressure distribution and circulation with the load cell. The lift forces that are calculated from pressure distribution is follow the similar trend with load cell lift forces. However, percentage difference is found to be less than 48%. On the other hand, lift forces that are calculated from circulation shows fluctuations at 10 and 12-degree angle of attack and reduced significantly at 20 and 30-degree angle of attack. The main reason for the fluctuation may be that we are calculated the pressure distribution by applying Bernoulli's equation at the surface. But for Bernoulli's theorem to be applicable, the flow should be steady and irrotational or if we

assume the thin boundary layer. However, in this application is rotational over an aerofoil and assumption may be wrong leads to higher fluctuations seen at various angle of attacks.

c) Table. 4 shows the pressure distribution variation with the angle of attack. The variation is initially seen to be increasing along the chord length until the angle of attack 12 degrees. On further increasing the angle of attack there is a decrease in the pressure distribution, this is due to decrease in the velocity over the upper surface therefore pressure increases on the upper surface because of Bernoulli's theorem and opposite trends follows on the lower surface. Finally, at the stall angle, i.e. the speed arrives to the minimum value for which flight can be sustained, hence, further increase of pressure over the upper surface reduces the lift force and the airfoil attains a decent motion as the flight can't be sustained.

d) The circulation increases with the increase of angle of attack as shown in Table (6). However, some fluctuations have been seen at various angle of attacks. This may be due to wrong assumption of calculation of velocity vector field from the pressure distribution. The numerical integration may also be the reason. We divided the aerofoil into 8 parts, by increasing the parts we can also increase the accuracy of the numerical integration.

e) The stall of an airfoil occurs at 30° angle of attack. This is also known as critical angle of attack. At stall angle, lift force increases but due to vortex shedding there are vibrations produced in the aerofoil and may lead to catastrophic failure. At stall angle, the drag force also increases due to flow separation occurs at the upper surface which disturbed the downwash and hence overall, increase in the drag force can be seen. The pressure distribution is maximum at the angle of stall. At angle of attack, the performance of the aerofoil decreases to significant level and catastrophic failure may occurs due to large drag force, vortex shedding.

f) Fig. (4) shows the variation of drag force with the increase with angle of attack. The drag force continues to increase with the angle of attack because of flow separation over the upper surface of an aerofoil. It follows the similar trend follows with variation of drag force shown in literatures. The Fig. (5) shows the variation of lift coefficient with the angle of attack. The general trend of lift coefficient shown in literatures is that lift coefficient increases with increase of angle of attack and maximum lift coefficient is found to at an angle of 12 or 13-degree angle after that it goes on decreasing with the further increase in the angle of attack. At stall angle, the lift coefficient also increases. From Fig. (5), the lift coefficient in case of pressure distribution increases and maximum value is found at angle of 12-degree and after that it decreases and then again increases at angle of attack. So, the overall trend is similar to literatures trend. However, some fluctuations can be seen on some angle of attack. These may be due to experimentation errors. While, the lift coefficient from circulation shows fluctuations, this may be due to the wrong assumption made for the calculation of velocity vector field. The load cell gives the most accurate results among the all three techniques because it is directly obtained from the instrument and no analytical calculations are involved. Pressure distribution also shows the good agreement with the literature. From the literature, the C_L/C_D first increases and attains the maximum value at 12-degree and goes on decreasing with the further increase in the angle of attack. From Fig. (6) all three method depicts similar trend however, the fluctuation in the results can be seen. But if we look at the overall scenario, the behaviour of the profiles of all the three method are same with literature.

References

[1] Saddiqi Kamran, lecture Notes on Aerodynamics, PP-2-6
[2] Airfoil Aerodynamics Lab Reference Sheet, PP 1-4
[3] Lab manual, University of Western Ontario, Aerofoil Aerodynamics, pp. 1-6